

NO INFORMATION WITHOUT DATA

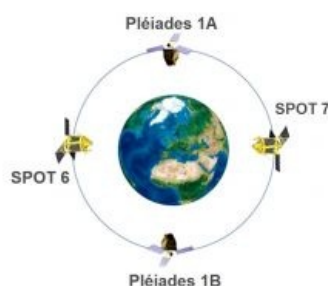
Recent Advances in Geodata Acquisition Technologies



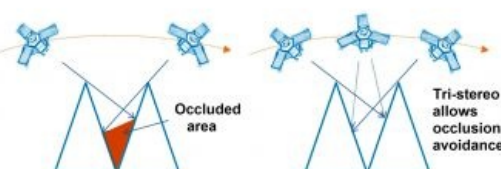
Today's geodata acquisition technologies combine microprocessors, computer power, solid state drives, complementary metal-oxide-semiconductor (CMOS) sensors, miniaturisation and many more developments. But demand is just as important as supply, and demand is rapidly increasing in our changing world. Read on for details of recent advances in geodata acquisition technologies.



In today's world, we are seeing metropolises cluster to form megalopolises, climate change threatens humans, land and livestock in low-lying areas such as river deltas and valleys, and massively populated areas are prone to earthquakes and landslides. All of these factors are increasing the demand for geodata acquisition.

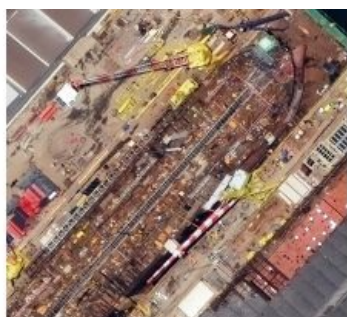


This article starts with total stations, continues with developments in GNSS positioning and navigation and proceeds with airborne Lidar and unmanned airborne systems (UASs). It then looks at the functionalities of point cloud processing software and the possibilities of dense image matching, before ending with recent advances in optical image sensors in space. The sources used include conference papers, brochures, factsheets, white papers, industry websites and Geo-matching.com, the product comparison website for hardware and software.



Total stations

A [total station](#) (TS) is a theodolite integrated with an electronic distance meter (EDM). The basic concept of using one device to measure distances and two angles – horizontal and vertical – has not changed over time (Figure 1). The revolution has taken place inside and stems from rapid technological advances which have boosted automation. Added to this, industrial designers are increasingly defining the look of total stations, with a prevalence of striking colours and robust lines. One day the dealer may ask: 'Where do you want me to fix your headshot?' Over time the basic components have been extended with many features being added to ease operation and reduce surveying costs. Stepless magnetic servomotors quickly and silently move the telescope along the horizontal and vertical. The surveyor just needs to aim the prism at the target and the telescope positions itself, which saves time when staking out coordinates. The prism is



pinpointed through either radio signals or imaging. Since radio links enable the device to be steered by a pole-mounted external controller, a robotic TS can be operated by one person alone. TSs require reference points for positioning and orientation. To meet this need a GNSS receiver can be mounted on top of the TS or on the prism pole. However, signals may be too weak in the vicinity of trees or buildings (Figure 2), in which case the total station takes over. This dual configuration increases the efficiency of massive data collection conducted by one person. A digital camera, mounted into the telescope coaxially with the optics and the EDM, allows snapshots documenting the site and notes to be written on the TS screen using a 'digital pencil'. This supports office-based processing, may avoid trips back to the field and allows the creation of orthoimagery. Imaging also enables the prism to be tracked and relocated when the connection is lost due to objects passing through the line of sight. Automatic target recognition allows automated deformation studies of dams and other structures. Terrestrial laser scanners (TLSs) have gained wide applications. A TLS and an EDM unit have much in common: a TLS operates without prism just as a TS can do, and both employ either pulsed laser or phase shifts. It therefore makes sense to extend a TS with the TLS ability to collect a point cloud. For example the Trimble S9, introduced in 2015, combines scanning, imaging and surveying. Depending on object reflectivity, the ranges vary from 1km to 2.2km.

GNSS receivers

The number of [GNSS satellites](#) is steadily growing. Galileo satellites numbers 5 and 6, named Doresa and Milena, were launched on 22 August 2014 but ended up in the wrong orbit. Two further Galileo satellites, numbers 9 and 10, lifted off on 11 September 2015, raising the number of satellites in the constellation to 10. One and a half months later, on 31 October 2015, the USA GPS constellation was enriched with the eleventh GPS IIF series satellite. IIF-12, the last of the series, has been scheduled for launch on 3 February 2016. The GPS IIF satellites feature a new third civil signal, L5, which provides improved signals and delivers higher accuracy through improved atomic clocks. To date, the GPS constellation consists of two GPS IIA's, 12 GPS IIRs, 7 GPS IIR-Ms and 11 GPS IIF satellites. Today's GNSS devices are able to track all four GNSS constellations that are either completed or still under development. Some are capable of tracking Quasi-Zenith Satellite System (QZSS) signals, a Japanese constellation which will consist of four satellites. QZSS is primarily aimed at increasing the number of GNSS signals in Japan's numerous urban canyons, where only satellites high above the horizon are in line of sight. The first – and so far the only – such satellite was launched on 11 September 2010. Survey-grade GNSS receivers allow access to satellite-based augmentation systems (SBASs) to support wide-area and differential GNSS. The publicly funded SBAS facilities for improving GNSS precision include: the Wide Area Augmentation System (WAAS) exploiting base stations widely distributed above the USA; the European Geostationary Navigation Overlay Service (EGNOS), the Japanese Multi-functional Satellite Augmentation System (MSAS) and India's GPS Aided Geo Augmented Navigation (GAGAN) technology demonstration system. To enable receipt of all the signals today's GNSS receivers are equipped to track up to hundreds of channels simultaneously (Figure 3).

Airborne Lidar

[Airborne Lidar](#) has matured into a mapping technology routinely used for 3D modelling of urban areas for capturing boreal forests, seabed mapping and many other uses. The frequency of firing laser pulses continues to soar and has reached over one million pulses per second. Multiple pulses in air and (full) waveform digitisation are other recent achievements and the possibilities for advancement are not yet exhausted. In December 2014 Optech introduced the world's first multispectral airborne Lidar: [Titan](#). Three independent pulses – wavelengths 532nm, 1064nm and 1550nm – are emitted, each with a 300kHz effective sampling rate for a combined ground sampling rate of 900kHz. The flying height for both topographic and bathymetric surveys is at least 300m while the maximum height over water is 600m and over land is 2,000m. The envisaged uses include topographic surveying, 3D land cover classification, environmental modelling, vegetation mapping and shallow water bathymetry. Since the three pulses do not follow the same path through air the footprints of the pulses do not hit the same spot, i.e. the reflection value of just one spectral band is assigned to one x,y position. The three reflections can be combined through gridding, which transfers to the point cloud to a raster. Riegl's [VQ-880-G](#) has been designed for combined topographic and bathymetric surveying. The measurement rate is up to 550kHz while 160 scans per second can be made. In March 2014 Swedish Airborne Hydrography AB (AHAB), which has been part of Leica Geosystems since October 2013, launched the [Dual Head](#) consisting of two scanners each emitting up to 500,000 pulses per second, totalling a pulse rate of 1MHz, and joined by an RCD30 80MP camera recording RGB and near infrared. When flying at a height of 1km, the point density is 16 points/m². The scan pattern is circular enabling the receipt of up to four returns per ground point. One sensor is pointing forward and one backward; the resulting oblique view enables the recording of facades on both sides of buildings. Bathymetry can be captured by two oblique systems: one for shallow water (max. depth 15m, pulse rate 35kHz) and one for deep water (max. depth 50m, pulse rate 10kHz); penetration depth depends on how clear the water is. Both systems can be combined with the [DragonEye](#) to seamlessly capture the seabed and adjoining land.

UASs

[Unmanned airborne systems](#) (UASs) have found use in many 2D and 3D mapping, inspection and monitoring tasks. They are steered by remote control or autonomously follow a pre-specified air path. The flight is guided by GNSS coupled with an IMU, and during processing GNSS and IMU data is used for georeferencing the sensor data. The sensors on board include RGB cameras, near-infrared (NIR) cameras, thermal infrared (TIR) sensors and Lidar. Some UASs allow two or more sensors as payload. In the *GIM International* UAS Special in 2014 I grouped UASs into two categories: fixed wings and multicopters. The first type uses the uplift abilities of wings, thus reducing energy consumption and remaining airborne for longer compared to a copter with the same dimensions. The wings allow high-speed flying and the capture of larger areas per flight. Copters can hover and, in contrast to fixed wings, need only small spaces for take-off and landing as they can ascend and descend vertically. Hence, a copter is ideally suited for capturing single buildings and small areas. Is the choice limited to either a fixed wing or a copter, as my tagging suggests? No, because a third type emerged recently: the hybrid UAS. Aerolution from Berlin has recently brought out the [Songbird 1400](#), which is basically a fixed wing but the four rotors are not mounted rigidly on the wings; instead, the blades can rotate from the vertical pose, which is normal for a fixed wing, to horizontal (Figure 4). The horizontal pose gives the fixed wing a vertical take-off and landing (VTOL) ability as if it were a copter. The UAS can stay in the air for over one hour, i.e. two to three times longer than a copter, provided that the copter facility is only used for launch and landing. Hovering and other copter-like manoeuvres consume copter-like energy, reducing air time. Meanwhile, the hybrid does not require a runway, catapult or parachute, which reduces the risk of damaging on-board sensors and other components.

Point clouds

A point cloud is a set of data points represented as a duplet of x,y coordinates, height/depth values and possible other attributes, including reflection intensities or RGB from a colour image. The x,y duplet and its attributes form the nucleus of the point cloud and the number of nuclei may run into billions. [Processing software](#) may be general purpose and handle point clouds from a diversity of sensors or may be dedicated to specific outputs from TLSs, airborne Lidars or mobile mapping systems, for example. Some packages are proprietary, developed to process the outputs of the manufacturer's sensors. A generic package able to handle all types of sensor output and to generate all types of end product does not yet exist. Vendors have recognised that clients need to process the outputs of their sensors and have complemented their hardware with proprietary software for managing, georeferencing, visualising, editing and exporting the outputs to dedicated software. Some software builders have spotted potential in offering tools for creating a pallet of end products from Lidar or other sensors possibly combined with pixel data, from pixel data alone or from sonar. Other packages stem from the application domains, e.g. constructors used to a CAD system started to appreciate TLS point clouds and asked vendors to add modules for processing them. Some manufacturers discovered new opportunities and built dedicated modules on top of one or more base modules aimed at, for example, the mining industry or 3D models of crash sites. This process is far from complete, and new tools are being added all the time. Before purchasing software, one should examine its functionalities as well as its design ideas, any current or planned extensions, its ability to join modules into one workflow and its interoperability with other software and services. Figure 5 categorises the functionalities.

DIM

Today's [photogrammetric software](#) enables high automation of the chain, from flight planning, self-calibration of consumer-grade cameras and aero triangulation up to the creation of DEMs and orthomosaics as well as their confluence: 3D landscape and city models. A recent development is dense image matching (DIM), which enables computation of a height or depth value for each and every pixel, thus producing high-resolution digital surface models (DSMs) and – by filtering out points reflected on buildings and vegetation – digital elevation models (DEMs) in automatic or semi-automatic workflows. The ground sampling distance (GSD) of the DSMs and DEMs is similar to the imagery from which they are derived, so that an image with a GSD of 5cm may deliver a density of up to 400 points/m². A package specifically for creating true orthos, DSMs and DEMs is called SURE, which has been developed at the University of Stuttgart and distributed through its spin-off [nFrames](#). Its core is a variation on the semi-global matching algorithm. Today, a variety of packages provide DIM facilities (Table 1).

Brand	Company	Country
3Dsurvey	Modri planet	Slovenia
Correlator3D	SimActive	Canada
DroneDeplo	DroneDeplo	USA
EnsoMosaic	MosaicMill	Finland
Inpho	Trimble	USA
Orbit Softcopy	Orbit	Belgium
Pix4Dmapper	Pix4D	Switzerland
Photomod	Racurs	Russia
RapidStation	PIEnengineering	Finland
SURE	nFrames	Germany
UnlimitedAerial	Meixner Imaging	Austria

Table 1, Photogrammetric software packages providing dense image matching (DIM) facilities (information partly sourced from Geo-matching.com).

High-resolution optical EO sensors

Over 200 optical [Earth Observation](#) (EO) satellites are in orbit, run by over 30 countries. France and the USA take the lead. The French SPOT 7 lifted off on 30 June 2014 and DigitalGlobe's WorldView-3 was launched on 13 August 2014. SPOT 7 completes the [constellation of four satellites](#) operating in the same orbit consisting of its twin sister SPOT 6 and Pléiades 1A and 1B. Each of the twins is phased 180° (Figure 6). The nadir revisit rate is 26 days, but the pointing agility allows each site to be captured once a day if SPOT 6 and 7 operate in conjunction and off-nadir areas to be captured on the same pass; the sensors can point to areas within a 1,500km-wide corridor. Through rapidly switching views up to 750km to the right or to the left of nadir, 11 scenes of 60km by 60km can be captured within an orbit segment of 1,000km. More than one target on the same pass at the same latitude can be captured too (Figure 7C), while elongated objects such as power lines, rivers or other corridors may be followed (Figure 7D). The agility enables along-track stereo images as well as tri-stereo. The latter reduces occlusions, thus improving DEM quality (Figure 8). The 12 bits (4,096 values) per band enable enhancement of details which suffer from overcast, (cloud) shadow or little texture such as dunes and ice. By default the images are oriented north to south, i.e. the scan lines are not perpendicular to nadir. To maintain the north to south direction the sensors have to be slowly moved away from nadir, but at a certain moment the sensors have to rotate to their start positions. Therefore, the maximum length of one north-to-south strip is 600km (Figure 7A, B). The incorporation of weather forecasts in the mission planning avoids capturing of scenes hidden by clouds. Table 2 shows spectral and spatial features of SPOT and Pléiades.

	SPOT 6 & 7	Pléiades 1A & 1B
Panchromatic	0.450 - 0.745	0.480 – 0.830
Blue	0.450 - 0.520	0.430 – 0.550
Green	0.530 - 0.590	0.490 – 0.610
Red	0.625 - 0.695	0.600 – 0.720
Near Infrared	0.760 - 0.890	0.750 – 0.950
Swath width	60km	20km
GSD Pan	1.5m	0.5m
GSD MS	6m	2m

Table 2, Spectral bands (μm), swath width and GSDs of SPOT 6 & 7 and Pléiades 1A & 1B.

WorldView-3 has the same spectral characteristics as [WorldView-2](#) (Table 3), launched 8 October 2009, but acquires the images with a higher GSD: 31cm instead of 46cm in the panchromatic (Pan) mode and 1.24m instead of 1.85m in the multispectral (MS) mode (Figure 9). All figures refer to nadir. WorldView-3 also adds to its spectral sensing abilities 8 shortwave infrared (SWIR) bands with a GSD of 3.7m and 12 CAVIS (Clouds, Aerosols, Vapours, Ice and Snow) bands with a GSD of 30m. The coverage capacity of WorldView-2 is 1 million km^2 per day, and for WorldView-3 this figure is 680,000 km^2 . In other words, increasing the GSD by a factor of 1.48 decreases the daily coverage by the same factor. The constellation of the four satellites with a GSD better than 50cm allows 60% of the Earth's surface to be captured monthly and intraday revisits of the same areas.

	μm
Pan	0.45 – 0.80
MS	
Coastal	0.4 – 0.45
Blue	0.45 – 0.51
Green	0.51 – 0.58
Yellow	0.585 – 0.625
Red	0.63 – 0.69
Red Edge	0.705 – 0.745
NIR1	0.77 – 0.895
NIR2	0.86 – 1.04

Table 3, Spectral bands of WorldView-2 and WorldView-3.

Concluding remarks

Data cannot be created out of thin air. To hearten those surveyors who may unfairly fear that their profession is in danger of extinction, I finish with a quote from Digital Globe: “You cannot create data from nothing and the laws of physics cannot be conquered via software enhancements.”

Biography of the Author

Mathias Lemmens gained a PhD degree from Delft University of Technology, The Netherlands, where he presently lectures on geodata acquisition technologies and geodata quality. He has been involved with *GIM International* since 1997, presently as senior editor. He is an international consultant and the author of the book *Geo-information: Technologies, Applications and the Environment* published by Springer in 2011.

Email: m.j.p.m.lemmens@tudelft.nl

Figure Captions

Figure 1, Evolution from theodolite to total station. From left to right: Wild T3, introduced 1925; Aga Geodimeter 14, manufactured 1970; EDM mounted on theodolite, HP 3820A; Leica FlexLine TS02plus (2013); Spectra Precision Focus 35 (2014); Ruide RIS and Trimble S9, both from 2015. (Courtesy: M. Lemmens)

Figure 2, Pole equipped with external controller, prism and GNSS (left) and GNSS antenna on top of total station. (Courtesy: Leica Geosystems)

Figure 3, Some of the GNSS receivers introduced in 2015 which can track hundreds of channels at the same time. (Courtesy: M. Lemmens)

Figure 4, Looking like a fixed wing, this hybrid UAS combines the pros of a fixed wing with the VTOL ability of a copter. (Courtesy: Aerolution)

Figure 5, Functionalities of point cloud processing software categorised in 8 main groups. (Courtesy: M. Lemmens)

Figure 6, SPOT 6 & 7 and Pléiades 1A & 1B operate in the same orbit, each phased 180°.

Figure 7, High agility allows various coverage scenarios. (Courtesy: Airbus Defence and Space, and M. Lemmens)

Figure 8, Difference between stereo and tri-stereo. (Courtesy: Airbus Defence and Space, and M. Lemmens)

Figure 9, This 40cm WorldView-3 image of a ship unloading in the docks of Rio de Janeiro, Brazil, shows the steel lattice structure of the cranes. (Courtesy: DigitalGlobe)

Further Reading

- Fleming, S., Woodhouse, I.H., Cottin, A. (2015) Bringing Colour to Point Clouds – Developments in Multispectral Lidar Are Changing the Way We See Point Clouds, *GIM International*, 29:2, pp. 22-25.
- Lemmens, M. (2014) Point Clouds (1) & (2), *GIM International*, 28:6, pp. 16-21 and 28:7, pp. 27-33.

